THE JOURNAL OF BIOLOGICAL CHEMISTRY
Vol. 273, No. 39, Issue of September 25, pp. 25320–25328, 1998

Printed in U.S.A.

Activation and Oligomerization of Aspartylglucosaminidase*

(Received for publication, April 13, 1998, and in revised form, July 16, 1998)

Jani Saarela‡, Minna Laine‡, Ritva Tikkanen§, Carita Oinonen¶, Anu Jalanko‡, Juha Rouvinen¶, and Leena Peltonen‡‖

From the ‡University of Helsinki, Department of Medical Genetics and National Public Health Institute, Department of Molecular Genetics, Mannerheimintie 166, FIN-00300 Helsinki, Finland and the ¶University of Joensuu, Department of Chemistry, P.O. Box 111, FIN-87101 Joensuu, Finland

Secretory, membrane, and lysosomal proteins undergo covalent modifications and acquire their secondary and tertiary structure in the lumen of the endoplasmic reticulum (ER). In order to pass the ER quality control system and become transported to their final destinations, many of them are also assembled into oligomers. We have recently determined the three-dimensional structure of lysosomal aspartylglucosaminidase (AGA), which belongs to a newly discovered family of homologous amidohydrolases, the N-terminal nucleophile hydrolases. Members of this protein family are activated from an inactive precursor molecule by an autocatalytic proteolytic processing event whose exact mechanism has not been thoroughly determined. Here we have characterized in more detail the initial events in the ER required for the formation of active AGA enzyme using transient expression of polypeptides carrying targeted amino acid substitutions. We show that His^{124} at an interface between two heterodimers of AGA is crucial for the thermodynamically stable oligomeric structure of AGA. Furthermore, the side chain of Thr^{206} is essential both for the proteolytic activation and enzymatic activity of AGA. Finally, the proper geometry of the residues His^{204}–Asp^{205} seems to be crucial for the activation of AGA precursor polypeptides. We propose here a reaction mechanism for the activation of AGA which could be valid for homologous enzymes as well.

N-terminal nucleophile hydrolases (Ntn hydrolases)[1] form a novel class of hydrolytic enzymes. They are activated from an enzymatically inactive precursor polypeptide by a proteolytic processing step in which one peptide bond is hydrolyzed, creating a new N-terminal residue. Several prokaryotic amidohydrolases belonging to the Ntn hydrolases have been described with very different substrate specificities and functions (1). Glutamine 5-phosphoribosyl-1-pyrophosphate amidotransferase (2), penicillin acylase (3), the proteasome β-subunit (4), and glucosamine-6-phosphate synthase (5) all have a similar central four-layer sandwich of α-helices and β-sheets (αββα) as a catalytic domain and an N-terminal nucleophile responsible for catalyzing the hydrolysis of an amide bond. The Ntn hydrolases display distinct structural similarity to human aspartylglucosaminidase (AGA), the structure of which we have recently determined to 2.0-Å resolution (6).

The N-terminal residue, which is exposed upon the proteolytic cleavage of the precursor polypeptide, has been shown to be essential for the enzymatic activity in the Ntn hydrolases. This residue is threonine in AGA and proteasome β-subunit, serine in penicillin acylase, and cysteine in glutamine 5-phosphoribosyl-1-pyrophosphate amidotransferase and glucosamine-6-phosphate synthase. All of these residues can function as a catalytic nucleophile and are located at the beginning of a β-strand. In the case of AGA and penicillin acylase activation, the precursor polypeptide chain is cleaved into two polypeptide subunits of the active protein, whereas in proteasome and glutamine 5-phosphoribosyl-1-pyrophosphate amidotransferase, the activation results in the removal of a propeptide. Recently, a number of studies have suggested that the breaking of this critical peptide bond occurs autocatalytically (7–11). Although there is no sequence similarity within the Ntn hydrolase family, all of the above mentioned amidohydrolases utilize a similar core structure for the amide bond hydrolysis in highly heterogenous substrates (6). It is therefore probable that the autocatalytic activation mechanism would be similar among different Ntn hydrolases, although comparative studies are still missing.

The only mammalian Ntn hydrolase whose crystallographic structure is known, aspartylglucosaminidase (glycosylasparaginase, N^4-(β-*N*-acetyl-D-glucosaminyl)-L-asparaginase; EC 3.5.1.26), is a lysosomal amidohydrolase that cleaves asparagine from the oligosaccharide as one of the final steps in the breakdown of glycoproteins (12). AGA is activated in the lumen of the endoplasmic reticulum (ER) from a single chain precursor by a cleavage that creates the 27-kDa pro-α- and 17-kDa β-subunits and exposes the active site N-terminal threonine in the beginning of the β-subunit (13). The active enzyme is a heterotetramer consisting of two α- and two β-subunits, and we have earlier suggested that dimerization of two precursor polypeptides actually precedes the proteolytic activation step (14). The maturation of AGA is completed in lysosomes where a small peptide is cleaved from the C terminus of both subunits (Fig. 1). The intracellular events allow easy monitoring for the lysosomal entry of the AGA polypeptides. AGA is transported into lysosomes via the mannose 6-phosphate receptor pathway, which is based on the recognition of the mannose 6-phosphate marker in the oligosaccharide chains of soluble lysosomal hydrolases by a specific receptor in the Golgi and consequent transport of the complex into a prelysosomal compartment. The mannose 6-phosphate marker is generated by a Golgi-resident enzyme, UDP-*N*-acetylglucosamine phosphotransferase, which recognizes lysosomal enzymes on the basis of a three-dimensional determinant in the protein. The phosphotransferase rec-

* The work was supported by The Ulla Hjelt Fund of the Pediatric Research Foundation, The Sigrid Juselius Foundation, and The Academy of Finland. The costs of publication of this article were defrayed in part by the payment of page charges. This article must therefore be hereby marked "*advertisement*" in accordance with 18 U.S.C. Section 1734 solely to indicate this fact.

§ Present address: Institute for Cell Biology, University of Bonn, Ulrich-Haberlandstrasse 61a, D-53121 Bonn, Germany.

‖ To whom correspondence should be addressed. Tel.: 358 9 47448393; Fax: 358 9 47448480; E-mail: Leena.Peltonen@ktl.fi.

[1] The abbreviations used are: Ntn hydrolase, N-terminal nucleophile hydrolase; AGA, aspartylglucosaminidase; CST, castanospermine; ER, endoplasmic reticulum; PAGE, polyacrylamide gel electrophoresis; WT, wild type.

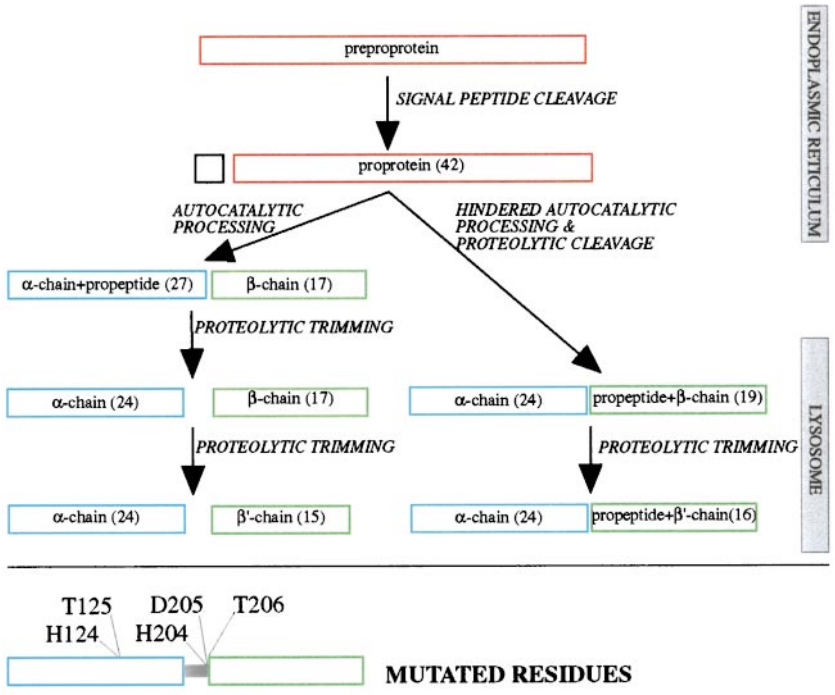

FIG. 1. **The processing of AGA.** The signal peptide is cleaved co-translationally in the ER from the AGA preproprotein, resulting in a monomeric precursor polypeptide (proprotein, shown in *red*). The normal autocatalytic processing pathway is represented on the *left*, and the abnormal nonactivating pathway caused by processing failure is on the *right*. The molecular weight determined from SDS-PAGE is shown in *parenthesis*. Two precursor molecules dimerize in the ER prior to the activation cleavage, which produces the two $\alpha\beta$ dimers of mature AGA (14). At the *bottom*, locations of the mutagenized amino acids are indicated *above* the pro-α- and β-subunits (drawn in *blue* and *green*, respectively). The cleaved peptide, which includes His^{204} and Asp^{205}, is shown in *gray*.

ognizes several distinct regions of native AGA that are located far apart at the surface of the molecule, and the phosphorylation of the oligosaccharides of AGA requires correct spatial position of these lysine-containing structures (15). Loss-of-function mutations in the human AGA gene lead to aspartylglucosaminuria (16). The majority of the mutations produce either a truncated polypeptide or cause defective folding and phosphorylation of the polypeptides (17).

This study was designed to obtain a more detailed understanding of the initial events upon the formation of the catalytically active AGA enzyme in the ER. By using site-directed mutagenesis we wanted to 1) characterize the dimerization of AGA and 2) define the amino acid residues critical for the autocatalytic activation mechanism itself.

EXPERIMENTAL PROCEDURES

Sequence Analysis—The amino acid sequences were retrieved using the Sequence Retrieval System at EMBL, and the program Gene-Works was used for sequence alignment.

Assay for AGA Activity—The AGA activity assay is based on colorimetric measurement of liberated *N*-acetylglucosamine and was performed as described earlier (17).

In Vitro Mutagenesis—Mutagenesis was performed with the Chameleon double-stranded, site-directed mutagenesis kit (Stratagene) as suggested by the manufacturer. As a template, we used the full-length coding region of AGA cDNA (18) cloned into the *Bam*HI site of mammalian expression vector SVpoly containing the SV40 early promoter. After mutagenesis, the insert was sequenced to exclude the possibility of unwanted mutations.

Transfection, Metabolic Labeling, and Immunoprecipitation—COS-1 cells were cultured in Dulbecco's modified Eagle's medium supplemented with 10% fetal calf serum. Transfections were performed with the DEAE-dextran/chloroquine method as described by Luthman and Magnusson (19). The cells were metabolically labeled or analyzed for AGA activity 72 h after transfection. Labeling with [^{35}S]Cys (Amersham Pharmacia Biotech) was performed as described earlier (18). The cells were labeled 1 h followed by a 1–24-h chase. Labeling with [^{32}P]orthophosphate (Amersham Pharmacia Biotech) was carried out for 2.5 h with 300 μCi of [^{32}P]P_i/ml, which was followed by a 3-h chase. For chaperone analysis, 1 mM castanospermine (CST; Boehringer Mannheim) was used in the culture medium 2 h before and during the labeling and chase periods. Immunoprecipitation was carried out using fixed *Staphylococcus aureus* cells (Immunoprecipitin, Life Technologies, Inc.; Pansorbin, Calbiochem) or protein A -Sepharose (Sigma) as described previously (20) using AGA-specific polyclonal antibody against the native enzyme (21). The labeled polypeptides were separated by 14% SDS-PAGE under reducing conditions (22). Endoglycosidase H (Boehringer Mannheim) digestion was performed as described previously (23).

Gel Filtration—For gel filtration experiments of *in vitro* expressed AGA polypeptides, 2.5×10^6 COS-1 cells were plated on a 10-cm cell culture dish and transfected with 20 μg of cDNA construct using the DEAE-dextran/chloroquine method. The cells were labeled with 200 μCi/ml [^{35}S]Cys for 1 h, chased for 3–6 h, and harvested with trypsinization. For mutant clones having a low expression level, two parallel transfections and labelings were performed at each experiment. The medium collected from the cells was concentrated to 150 μl with Centrex UF-2 30-kDa microconcentrators (Schleicher & Schuell). Gel filtration on a Superdex 75 (10/30) column (Amersham Pharmacia Biotech) was performed as described by Riikonen *et al.* (14). AGA polypeptides were immunoprecipitated from the collected fractions and analyzed by SDS-PAGE and fluorography.

RESULTS

Two Clusters of Conserved Residues—The amino acid sequences of glycoasparaginases and asparaginases were aligned (Fig. 2). Based on the information of the three-dimensional structure of human aspartylglucosaminidase, we analyzed the conservation of the active site, lysosomal targeting, and glycosylation residues among nine species. The important residues, regarding the AGA enzyme activity, are conserved from bacteria to mammals. This alignment reveals only 10% overall sequence identity (33 residues), while the catalytic Thr^{206} is absolutely conserved. Based on the alignment, we observed that there were two clusters in the three-dimensional structure of the native human AGA in which amino acids show high conservation (Fig. 3, *B* and *C*). One of these regions is located on the interface between the two $\alpha\beta$ dimers, and another is located on the active site area, suggesting functionally essential roles for these areas of the molecule. These regions were selected as targets to *in vitro* mutagenesis followed by functional analysis of polypeptides coded by the mutagenized cDNAs.

In Vitro Expression of Mutagenized AGA cDNA Constructs—*In vitro* mutagenesis was performed using the SVpoly vector containing human AGA cDNA as a template. The mutant plasmids were transfected into mammalian COS-1 cells, and the expressed polypeptides were metabolically labeled

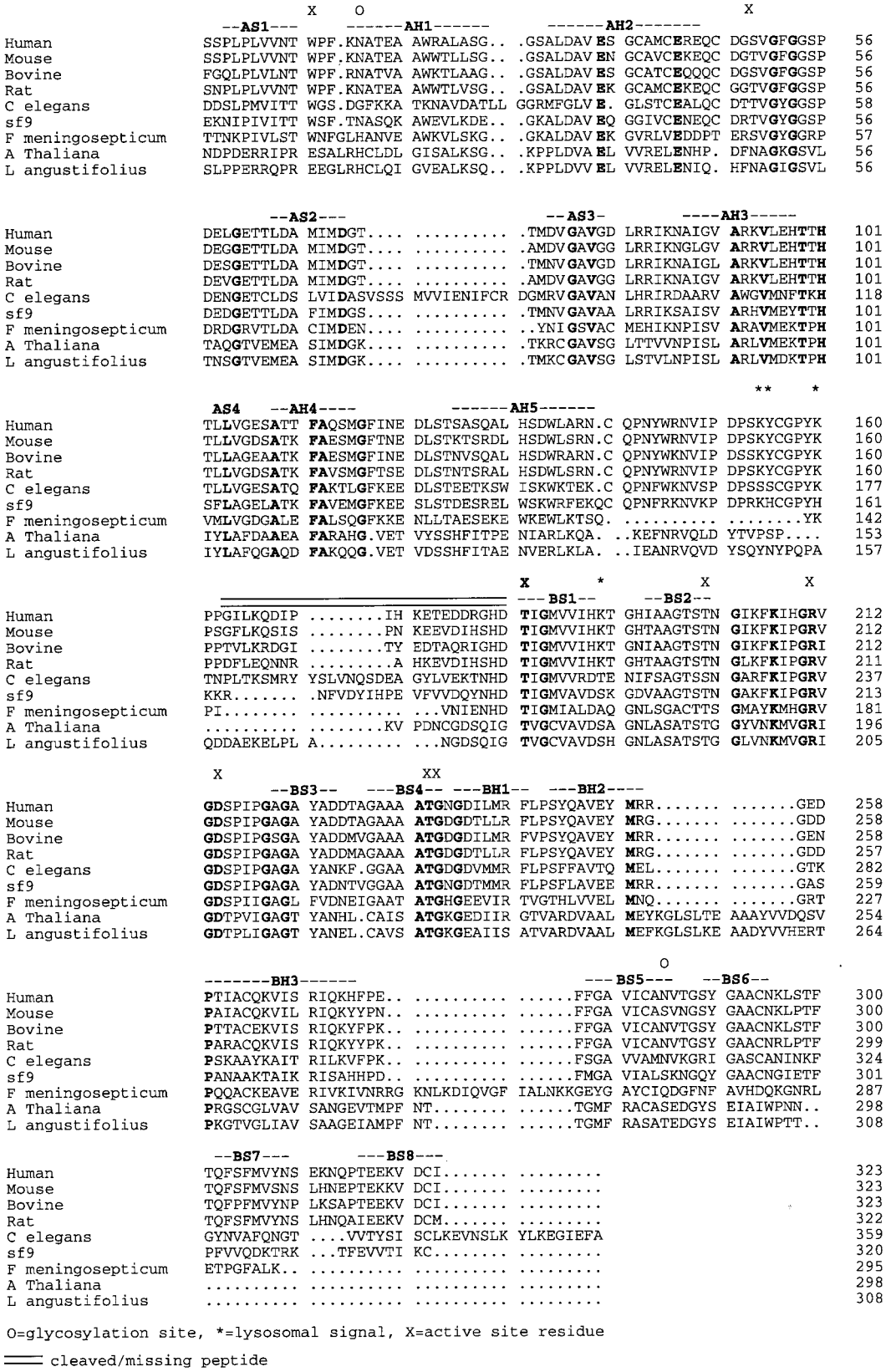

FIG. 2. **Amino acid sequence alignment of glycoasparaginases and asparaginases from different species.** The amino acid sequences were retrieved with the Sequence Retrieval System and aligned according to functional residues of the human AGA polypeptide sequence with the program Gene-Works. The functional residue symbols are explained *below* the alignment, and the conserved amino acids are in *boldface type*. The signal sequence of AGA, 23 amino acids, is not included here. Therefore, the active site Thr^{206} corresponds to Thr^{183} in this *figure*. The aligned species were human, mouse, bovine, rat, *Caenorhabditis elegans, Spodoptera frugiperda* (Sf9), *Flavobacterium meningosepticum, Arabidopsis thaliana*, and *Lupinus angustifolius*.

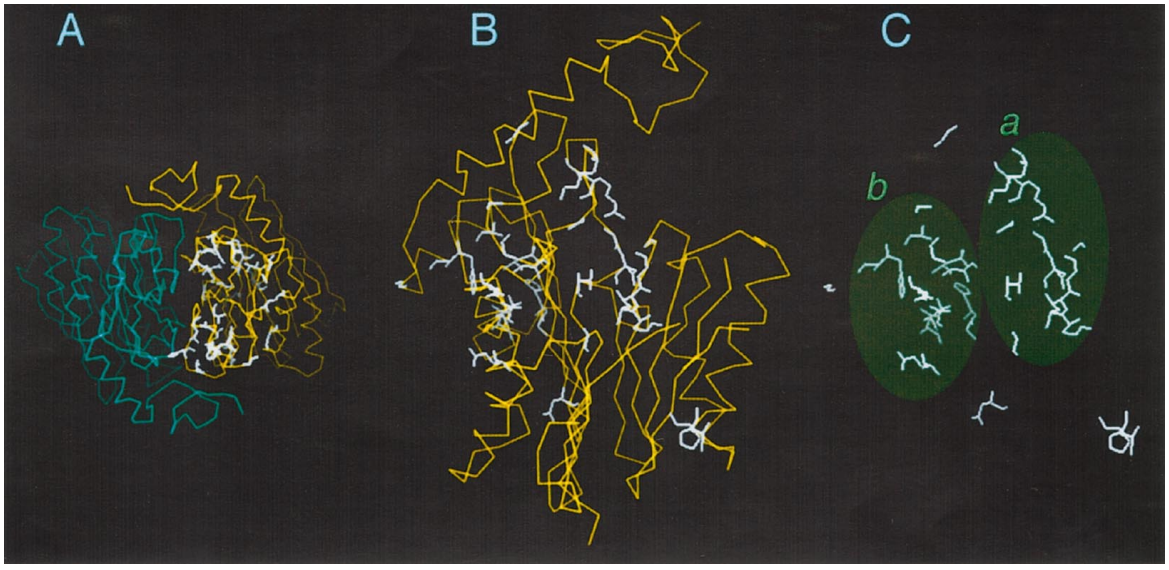

FIG. 3. **The conserved amino acid residues of AGA.** The alignment was constructed using reported glycoasparaginase and asparaginase amino acid sequences. The conserved amino acid residues are shown in *white*. *A*, the AGA molecule, consisting of two identical $\alpha\beta$ heterodimers (dimers are drawn in *light green* and *yellow*); conserved amino acid residues are drawn in one dimer. *B*, enlargement of an $\alpha\beta$ heterodimer. *C*, the conserved amino acids represented in Fig. 3*B* are located in two regions, which are depicted with *ovals*. The *a region* contains the active site residues of AGA. The *b region* contains residues on the packing interface between the two $\alpha\beta$ dimers. Only five residues lie outside these two regions. The image was made with the program XtalView (33).

TABLE I

Summary of analyzed substitutions: the substitutions of His^{124} and Thr^{125} located at the interface between the two $\alpha\beta$ dimers of AGA

The effect of selected amino acid substitutions on the processing of [^{35}S]Cys-labeled AGA polypeptides was determined by analyzing the samples by SDS-PAGE under reducing conditions. The first column represents the clones analyzed; amino acid names are in one-letter abbreviations. The second column represents the observed polypeptides in the cells (c) and medium (m); polypeptides are named as in Fig. 1. The expression level was calculated as the sum of densitometric scanning of autoradiographs from lysed cells and concentrated medium and is given as the percentage of the WT clone. The secretion level was calculated as the fraction of the secreted polypeptides from the total polypeptides as determined by densitometric scanning of autoradiographs. The intracellular activity was correlated to the expression level of the corresponding mutant, and the value is given as the percentage of the WT clone. The dimerization status of the precursor polypeptide, which was analyzed as described under "Experimental Procedures," is reported in the last column. Total protein concentration of cell lysates was determined to ensure that the number of cells in each experiment was equal (data not shown).

Clone	Polypeptides in the cells (c) and medium (m)					Expression level	Secretion	Activity in the cells	Dimerization of the precursor polypeptide
	Prec	Pro-α	α	β	β'				
						% WT	*% total*	*% WT*	
WT	c,m	c,m	c	c,m	c	100	46 ± 7	100	Dimer
COS						BG[a]	30 ± 3	BG	ND[b]
H124S[c]	c,m	c,m	c	c,m	c	211 ± 11	39 ± 2	43	Dimer
H124R	m					7 ± 1	100	PF[d]	Dimer + monomer
H124W	m					7 ± 1	100	PF	Dimer + monomer
T125A	c,m	c,m	c	c,m	c	120 ± 5	44 ± 1	68	Dimer
T125Y	c,m	c,m	c	c,m	c	33 ± 5	29 ± 7	75	Dimer
T125C	c,m	c,m	c	c,m	c	148 ± 10	51 ± 4	70	Dimer

[a] BG, background.
[b] Not determined.
[c] pCD-X expression vector.
[d] PF, processing failure.

with [^{35}S]Cys and/or [^{32}P]P_i. The labeled polypeptides were immunoprecipitated with a polyclonal antiserum raised against native AGA and separated by SDS-PAGE under reducing conditions, and the results were verified with analysis of total AGA protein by Western blotting. In addition, all mutant polypeptides were metabolically labeled with [^{35}S]Cys and chased for 1, 3, 6, and 24 h to monitor their intracellular processing and lysosomal targeting (data not shown). To analyze the dimerization event, the cell culture medium was gel-filtrated, and fractions corresponding to the molecular masses of labeled polypeptides between 125 and 20 kDa were collected and immunoprecipitated. The numeric values of expression level, secretion, and activity (activity being corrected with the expression level) were measured for each mutant (Tables I and II).

Substitutions at the Dimer Interface—We focused the production of amino acid substitutions on two molecular regions: 1) the dimer interface and 2) the autocatalytic processing site (Fig. 4). The dimer interface of AGA is a relatively wide area containing a number of hydrophobic residues. In the three-dimensional structure, the interface is quite flat except for one clear protrusion of a loop in one $\alpha\beta$ dimer that penetrates into the other $\alpha\beta$ dimer of the native enzyme. In this loop region, His^{124} is completely conserved and Thr^{125} is conserved in mammals. Arginine and tryptophan substitutions were produced for His^{124}, and alanine, tyrosine, and cysteine substitutions were produced for Thr^{125}. In addition, the H124S construct previously cloned into the pCD-X expression vector was analyzed (13). As a general practice, the replacing residues were chosen to be of equal size or smaller than the original residue so that the packing of the molecule should not be disturbed. This practice was not followed with H124R, H124W, and T125Y

TABLE II

Summary of analyzed substitutions: substitutions at the subunit processing site, where His^{204} and Asp^{205} precede the scissile Asp^{205}-Thr^{206} peptide bond

The effect of selected amino acid substitutions on the processing of [^{35}S]Cys-labeled AGA polypeptides was determined by analyzing the samples by SDS-PAGE under reducing conditions. The first column represents the clones analyzed; amino acid names are in one-letter abbreviations. The second column represents the observed polypeptides in the cells (c) and medium (m); polypeptides are named as in Fig. 1. The expression level was calculated as the sum of densitometric scanning of autoradiographs from lysed cells and concentrated medium and is given as the percentage of the WT clone. The secretion level was calculated as the fraction of the secreted polypeptides from the total polypeptides as determined by densitometric scanning of autoradiographs. The intracellular activity was correlated to the expression level of the corresponding mutant, and the value is given as the percentage of the WT clone. The dimerization status of the precursor polypeptide, which was analyzed as described under "Experimental Procedures," is reported in the last column. Total protein concentration of cell lysates was determined to ensure that the number of cells in each experiment was equal (data not shown).

Clone	Polypeptides in the cells (c) and medium (m)						Expression level	Secretion	Activity in the cells	Dimerization of the precursor polypeptide
	Prec	Pro-α	α	Pro-β	β	Pro-β′				
							% WT	*% total*	*% WT*	
H204G	c,m	c,m	c	c	c,m	c	76 ± 13	30 ± 3	30 + PF[a]	Dimer
H204S[b]	c,m	c,m	c	c	c,m	c	113 ± 2	29 ± 1	30 + PF	Dimer
D205G	c,m		c	c		c	87 ± 8	24 ± 3	PF	Dimer
D205A	c,m		c	c		c	54 ± 10	28 ± 6	PF	Dimer
D205S	c,m		c	c		c	67 ± 8	20 ± 2	PF	Dimer
H204G/D205G	c,m		c	c		c	62 ± 11	17 ± 2	PF	Dimer
H204I/D205G	c,m		c	c		c	87 ± 1	20 ± 2	PF	Dimer
T206C	c,m		c	c		c	66 ± 7	36 ± 4	PF	Dimer
T206A	c,m		c	c		c	105 ± 5	19 ± 3	PF	Dimer

[a] PF, processing failure.
[b] pCD-X expression vector.

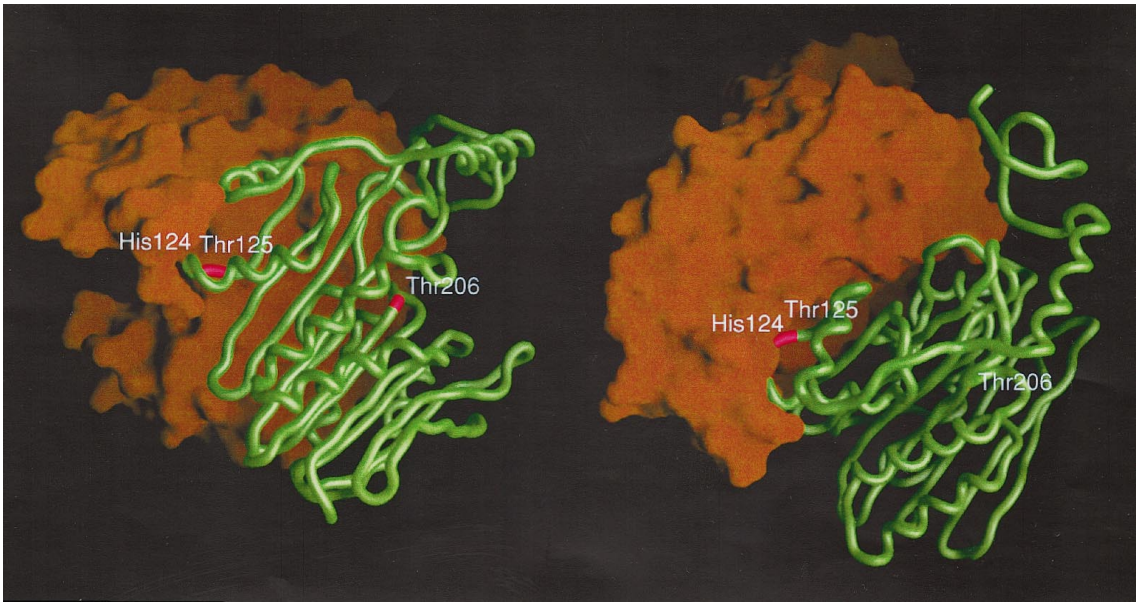

FIG. 4. **Image of the AGA molecule displaying the substituted amino acids.** One of the αβ dimers of AGA is drawn in *brown* as a molecular surface, while the other αβ dimer is drawn as a *green* polypeptide backbone. The substituted amino acids are shown in *red*, and the amino acid numbers are adjacent to the residues. His^{204} and Asp^{205} are not visible, because they are located in the polypeptide removed in the processing of the pro-α subunit and thus not present in the mature AGA structure. The narrow active site funnel of AGA is visible in the *middle* of the vertical surface of both αβ dimers on the *left* image. The image was made with the program Grasp (34) and rendered with Photoshop.

replacements in which we introduced a bulkier side chain in order to study whether a residue occupying more space affects the dimerization of precursor polypeptides.

Two substitutions were found to affect the dimerization of AGA, namely H124R and H124W. In the case of H124R and H124W mutants (shown for H124R, Fig. 5), the original amino acid side chain is replaced by a larger one. Due to a processing failure, these mutants produced only the nonprocessed precursor polypeptide, which was secreted to the culture medium, and thus no enzyme activity beyond the background level was detected. Both of these substitutions affected the dimerization of the precursor molecules, and both dimeric and monomeric precursor could be observed after gel filtration (shown for H124R, Fig. 6). H124R- and H124W-transfected cells produced only precursor polypeptides into the culture medium, indicating that the processing was completely prevented. However, when labeled with [^{35}S]Cys and [^{32}P]P_i, the oligosaccharides of mutant precursors were found to be normally phosphorylated (Fig. 7). This would suggest that these substitutions do not result in severe misfolding of AGA in the ER, since only correct positioning of the three phosphotransferase recognition regions results in the phosphorylation of the oligosaccharides of AGA (15). Since no polypeptides could be detected intracellularly in metabolic labeling experiments, immunofluorescence analysis of cells expressing H124R and H124W mutants was performed. This analysis revealed retention of AGA polypeptides in the Golgi and ER, which were intensively immunostained. Western blotting using antibodies against denatured subunits of AGA further demonstrated that a small quantity of degradation products existed intracellularly, suggesting slight instability of

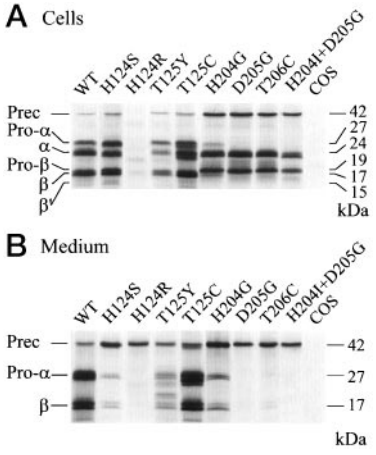

FIG. 5. **SDS-PAGE analysis of the processing of the WT AGA and mutated polypeptides.** COS-1 cells transfected with different AGA cDNA constructs were labeled with [^{35}S]Cys for 1 h and chased for 3 h. The labeled cells were lysed, and the polypeptides were immunoprecipitated using polyclonal antibodies against native AGA. The samples were analyzed by 14% SDS-PAGE under reducing conditions. *A*, intracellular processing of representative mutants. *B*, secreted polypeptides analyzed from the concentrated medium. Two glycosylation forms of polypeptides are often seen in gels, representing heterogeneity of the oligosaccharide chain. One-letter abbreviations of amino acid names are used, and the polypeptides are named according to Fig. 1. *Prec*, precursor polypeptide. The corresponding molecular masses were determined with molecular mass standards.

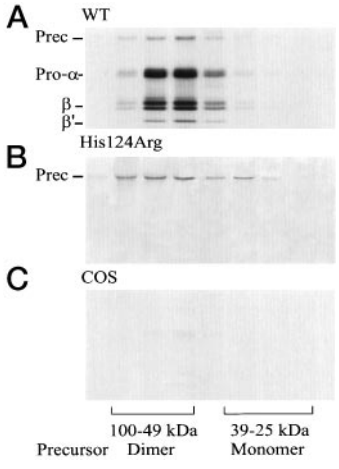

FIG. 6. **SDS-PAGE analysis of the gel-filtrated AGA polypeptides.** [^{35}S]Cys-labeled secreted polypeptides were concentrated from the medium and gel-filtrated with a Superdex 75 column. Fractions corresponding to polypeptides with molecular weights between 125 and 20 kDa were collected and immunoprecipitated using antibodies against native AGA. Samples were analyzed by 14% SDS-PAGE under reducing conditions. WT AGA (*A*), H124R (*B*), and COS cells (*C*), representing background, were labeled with [^{35}S]Cys.

the AGA polypeptides carrying these substitutions. However, when His^{124} was replaced with serine, which has a small side chain compared with histidine, arginine, and tryptophan, the dimerization or activation of the precursor polypeptides was not affected (Fig. 5).

T125Y mutant produced polypeptides comparable with the WT (Fig. 5), but the expression levels were only 33% of the WT as determined by scanning of autoradiographs (Table I). The low expression level was not a result of low transfection efficiency as confirmed by immunofluorescence analysis of T125Y-transfected cells (data not shown). In addition, Western blotting using antibodies against the denatured subunits of AGA demonstrated that WT levels of subunits existed intracellularly and that large quantities of the precursor polypeptide were

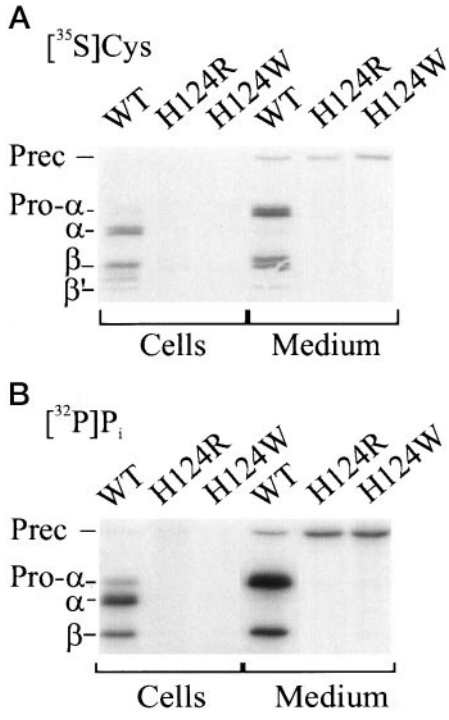

FIG. 7. **SDS-PAGE analysis of intracellular and secreted AGA polypeptides labeled with [^{35}S]Cys or [^{32}P]P$_i$.** [^{35}S]Cys- (*A*) and [^{32}P]P$_i$-labeled polypeptides (*B*) were immunoprecipitated from the lysed cells and from the concentrated medium. Polypeptides were analyzed as described in Fig. 5.

secreted. T125Y substitution did not affect the dimerization of precursor molecules.

The construct carrying the T125C substitution was expressed efficiently (Table I), and the mutant produced polypeptides with slightly higher electrophoretic mobility in SDS-PAGE in addition to the normal pro-α- and α-subunits (Fig. 5). Endoglycosidase H digestion showed that this was not due to differences in glycosylation (data not shown). The β-subunit was expressed in two different glycosylation forms, corresponding to the sizes of the WT β-subunit, and the difference in electrophoretic mobility in SDS-PAGE disappeared after the cleavage of oligosaccharides by endoglycosidase H digestion. This would suggest that partial misprocessing of the precursor polypeptide caused the existence of the extra α polypeptides. T125C substitution did not affect the dimerization of precursor molecules. Moreover, T125A substitution introduced an amino acid with a smaller side chain incapable of hydrogen bonding and was found to affect neither the processing nor the dimerization of AGA precursor polypeptides.

Substitutions at the Subunit Processing Site—During the autocatalytic activation of AGA, the peptide bond between Asp^{205} and Thr^{206} is cleaved. At this site, we mutagenized three residues: His^{204} and Asp^{205} before the cleavage site and Thr^{206} immediately after the cleaved bond. Thr^{206} is the catalytic residue in mature AGA, and it is completely conserved among the known glycoasparaginases and asparaginases. His^{204} and Asp^{205} are conserved in all aligned species except in plants. Both His^{204} and Asp^{205} were individually replaced by glycine, and a double substitution H204G/D205G was generated in order to study the role of possible strain of the polypeptide backbone in the activation process. The H204S construct previously cloned into the expression vector pCD-X was also analyzed (13). In addition, D205A and D205S substituted constructs were generated, and the active site Thr^{206} was replaced with cysteine and alanine. Finally, a construct carrying the substitutions H204I/D205G was produced in order to analyze if

the plant sequence could replace the conserved sequence of the human AGA polypeptides in the proteolytic activation.

The H204G- and H204S-transfected cells produced a large quantity of precursor polypeptide that became efficiently secreted. Only these two mutants at the processing site resulted in partial activation of AGA (shown for H204G, Fig. 5). Intracellularly, only small quantities of normal pro-α- and β-subunits existed, while larger amounts of α- and abnormal pro-β-subunits were produced due to inhibition of activation cleavage and normally occurring lysosomal processing (Fig. 1). The activity, 30% of the WT, can be accounted for by the normally processed portion of the β-subunit polypeptides. Similar processing has been described previously with the aspartylglucosaminuria-causing S72P substitution, which prevents the proteolytic activation cleavage of AGA precursors (17). Dimerization of the precursor polypeptides was not affected by His^{204} substitutions, which was the case for all Asp^{205} and Thr^{206} substitutions at the subunit processing site as well.

All produced Asp^{205} and Thr^{206} substitutions prevented the ER activation cleavage of the dimeric precursor molecule (shown for D205G and T206C, Fig. 5). The precursor polypeptide was not normally processed into subunits in the ER (Fig. 1); thus, all mutants were inactive, and abnormal pro-β and pro-β' were the only forms of the β-subunit present (Table II). The precursor polypeptide was transported into lysosomes, where a cleavage produced the α- and pro-β-subunits. Only the precursor polypeptide of Asp^{205} and Thr^{206} mutants was secreted to the medium. Similar processing has been reported with substitutions for amino acids Arg^{234} and Thr^{257} (11).

The plant sequence Ile^{204}-Gly^{205} was not functional in the activation of the human AGA polypeptides. The H204I/D205G double mutant was not processed and hence was totally inactive (Fig. 5). While H204G and H204S mutants had some enzyme activity, both the H204I/D205G and H204G/D205G double mutants were totally inactive, suggesting that D205G was responsible for the complete inactivation of the double mutant enzymes. The results indicate that Asp^{205} and Thr^{206} are essential for AGA activation, and substitutions of these amino acids systematically result in the processing failure described above.

In summary, two substitutions for His^{124} severely affected the dimerization of AGA precursor polypeptides, whereas substitutions for Thr^{125} did not have any effect on the dimerization. All substitutions for the proteolytic cleavage site affected the activation of AGA, and neither of the double mutants nor any of the Asp^{205} and Thr^{206} mutants were capable of activation.

We wanted to exclude the effect of overexpression on the results obtained, and stable CHO cell lines producing the H124R and T206C mutant AGA polypeptides were constructed. These mutants were selected for further analysis, since in COS-1 cells, H124R produced monomeric and T206C dimeric precursors. The results obtained with WT AGA-producing stable CHO cells were in good agreement with the results obtained with COS-1 cells. In addition, H124R and T206C mutants produced polypeptides equal to those detected in COS-1 cells (data not shown). The findings in the stable expression system confirmed the results obtained with transient expression in COS-1 cells.

The Effect of Calnexin and Calreticulin Chaperones on the Processing of AGA—Calnexin and calreticulin are molecular chaperones that only bind to monoglycosylated trimming intermediates of glycoproteins in the ER and promote correct folding (24). To monitor if AGA interacts with them, co-immunoprecipitations of metabolically labeled AGA and calnexin or AGA and calreticulin polypeptides were performed using antibodies against calnexin, calreticulin, or AGA. 5–60-min labeling for a stable CHO-WT-AGA cell line was used, but no AGA polypeptides were co-precipitated with calnexin or calreticulin antibody, and *vice versa* (data not shown). To confirm the preliminary result, the binding of glycoproteins to calnexin and calreticulin was inhibited using a glucosidase inhibitor, castanospermine (CST) before and during the labeling. CST prevents the cleavage of the two outermost glucose residues from the oligosaccharide by ER glucosidases I and II, thus inhibiting the binding of calnexin and calreticulin to glycoproteins (25, 26). The inhibition of calnexin and calreticulin had no effect on the processing of AGA. The only difference caused by CST was seen in the glycosylation of AGA subunits. This difference in the migration of AGA polypeptides in SDS-PAGE disappeared using endoglycosidase H digestion (Fig. 8).

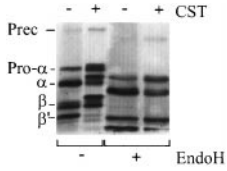

FIG. 8. **SDS-PAGE analysis of labeled WT AGA polypeptides expressed during castanospermine treatment.** WT AGA polypeptides, expressed in stable CHO-K1 cells, were labeled with [^{35}S]Cys using 1 mM CST during labeling and chase periods. Control samples were labeled without CST treatment. Immunoprecipitation using antibodies against native AGA was followed by endoglycosidase H digestion, which removes oligosaccharides from polypeptides. Samples were separated by 14% SDS-PAGE under reducing conditions.

DISCUSSION

Folding and Dimerization of AGA Polypeptides—The amino acid sequence comparison of nine different glycosylasparaginases and asparaginases revealed a total of 33 identical residues. When these residues were mapped on the three-dimensional structure of AGA, two clusters of conserved residues could be identified. One of them consists of the active site residues, and another is located in the structure that is packed against another $\alpha\beta$ dimer of the mature heterotetrameric AGA molecule (Fig. 3).

The calnexin and calreticulin chaperones interacted at the most only weakly with AGA, since the processing of AGA was not affected by the inhibition of calnexin and calreticulin interaction. This inhibition by CST is not complete, as concluded by Simons *et al.* (27), which could account for the small amount of normally sized α- and β-subunits observed (Fig. 8). However, the interaction of calnexin and calreticulin with influenza hemagglutinin has been determined by Hebert *et al.* (24) to be indispensable for the folding and oligomerization of this trimeric protein in microsomes. AGA is apparently not absolutely dependent on calnexin and calreticulin, since it is folded and oligomerized in the ER, while other chaperones may still be involved.

The phosphorylation of mutant polypeptides with defective dimerization, namely H124R and H124W, was found to be normal (Fig. 6 and 7). AGA is phosphorylated only as a structure consisting of two $\alpha\beta$ dimers or two precursor molecules (15). Therefore, this would suggest that once these mutant AGA precursor molecules were properly folded in the ER, they were dimerized and transported to the Golgi to be phosphorylated. However, the activation cleavage in the ER did not occur with H124R and H124W mutants, and no polypeptides were detectable intracellularly in autoradiographs. Immunofluorescence analysis of intracellular AGA polypeptides in H124R and H124W mutant-transfected cells revealed staining of the Golgi and ER, implying that even at steady state, the mutant AGA polypeptides were not present in lysosomes. Western blotting

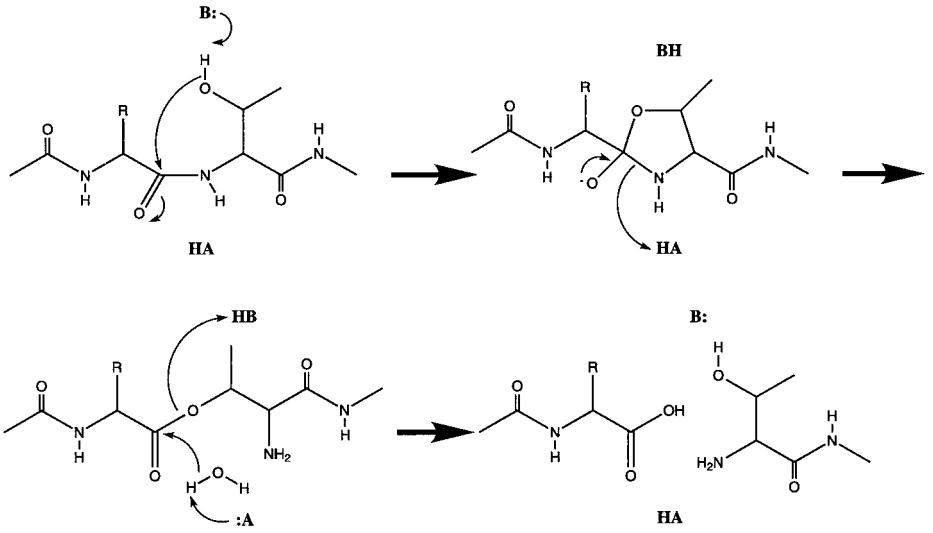

FIG. 9. **The proposed autocatalytic activation mechanism of AGA.** The side chain hydroxyl group of Thr^{206} forms a covalent bond to the carbonyl carbon of Asp^{205}. This is possibly assisted by a general base (*B*), which captures the proton of the hydroxyl group of Thr^{206}, and a tetrahedral intermediate is formed. In the next step, the C–N bond is broken, and a general acid (*HA*) donates a proton to the newly formed amino group terminal. This is followed by a water attack to the carbonyl carbon, and the bond between the carbonyl carbon of Asp^{205} and the side chain oxygen of Thr^{206} is broken. A tetrahedral intermediate similar to the one described above may exist after the water attack.

analysis showed small quantities of degraded subunits, indicating that the amount of steady state polypeptides was low most probably because of instability caused by monomerization. The folding of the polypeptides was probably not disturbed by substitutions for His^{124}, since the *N*-linked oligosaccharides were normally phosphorylated. Correct folding is further supported by the fact that the most common mutation causing aspartylglucosaminuria, AGU_{Fin}, prevents the correct folding of the C-terminal end of the α-subunit (6, 18), and the mutant polypeptides are not phosphorylated *in vitro* (17).

When His^{124} was substituted with an amino acid having a bulky side chain, the dimerization of precursor molecules was severely affected. The bulky side chain of arginine or tryptophan obviously did not fit properly into the narrow gap between the two precursor molecules, since both H124R and H124W substitutions affected dimerization. However, H124S substitution introduced an amino acid with a small side chain, which is not capable of forming the hydrogen bonds that His^{124} makes. This replacement did not affect the dimerization or activation of the AGA precursor polypeptides. Therefore, His^{124} seems to be crucial for the correct packing of two precursor polypeptides against each other, as suggested by the crystal structure.

In the case of T125Y, larger quantities of AGA polypeptides were detectable by Western blot analysis than by immunoprecipitation. This would suggest that a significant fraction of the polypeptides became misfolded and unstable. Abnormally sized subunits present in the culture medium possibly represent degradation products of the polypeptides. However, in the case of T125C, the overall folding of polypeptides was correct, and they were recognized by the native AGA antibody. The α-subunit was present in two slightly different forms probably due to partial misfolding and consequent misprocessing of the polypeptides. These Thr^{125} mutants therefore showed a relatively minor effect on the processing of the polypeptides and did not affect the dimerization of precursors. Finally, the T125A substitution did not affect dimerization or activation of the precursor polypeptides.

Processing of the AGA Precursor Polypeptide—The sequence His^{204}-Asp^{205}-Thr^{206} at the proteolytic activation site is conserved in most of the currently characterized glycoasparaginases or asparaginases (Fig. 2). However, plant asparaginases do not have the His-Asp-Thr but rather a Ile-Gly-Thr sequence. Although there are probably small differences in the three-dimensional structure, it is very likely that the overall structure of plant enzymes is similar to the human AGA. Because the active site residues participating in catalysis are identical, the enzymatic reaction mechanism is probably similar. It is highly probable that the activation mechanism of all these enzymes is also similar, but the lack of complete conservation would suggest that side chains of the amino acid residues before the cleavage point are not directly participating in the autocatalytic activation in (glyco)asparaginases.

When the human activation sequence was replaced with the one from the plants, the activation cleavage was totally prevented. This is not surprising, because the overall amino acid identity is only 25% between the human and plant sequences. In addition, the human glycoasparaginase and the plant asparaginases have different substrates. Therefore, the active site funnels of the human and plant enzymes are probably somewhat different in three-dimensional structure, and the interactions between the activation site residues and the neighboring residues are not identical. This is supported by the fact that the folding of the bacterial glycosylasparaginase is very similar to the human AGA, although the sequence identity is quite low and disulfide bridges are not present in the bacterial enzyme (28). The structure reveals that the active site funnel is wider in the bacterial than in the human AGA enzyme, although the active site residues are conserved.

In human AGA, the Asp^{205}-Thr^{206} sequence seems to be definitively required for the activation. Both Thr^{206} mutants as well as all Asp^{205} mutants completely prevented the activation cleavage of precursor molecules, producing the abnormal pro-β-subunit. In contrast to previous studies (8, 29), our results demonstrate that Thr^{206} is required for the actual proteolytic activation of the precursor polypeptide, in addition to its role in the catalytic activity of AGA (6). The requirement of an equivalent threonine in the β-subunit of 20 S proteasome processing and activity has been reported as well (9, 10). However, when Thr^{206} of human AGA was replaced by serine, the activation cleavage occurred, but the mutant enzyme was inactive (30). These results indicate that the hydroxyl group of Thr^{206} or Ser^{206} side chain is actually required for activation, but only in Thr^{206} is this hydroxyl group in correct position for enzymatic catalysis of glycoasparagine breakdown.

Guan *et al.* (8) suggested that His^{204} (numbered as His^{150} in the bacterial AGA) would be necessary for the initiation of the nucleophilic attack resulting in the activation of bacterial AGA. In contrast, our results suggest that His^{204} is not absolutely required for the cleavage reaction, since H204G and H204S mutant precursor polypeptides were activated to some extent. Moreover, H204S precursor polypeptide has been demonstrated to be cleaved, probably autocatalytically, in the me-

dium (17). In this case, the cleavage was independent of serum or protease inhibitors. Furthermore, the sequence alignment (Fig. 2) supports the argument that His^{204} is not necessary for the AGA activation cleavage.

Substitutions of the completely conserved residue Thr^{206} hindered the processing, suggesting that the side chain of Thr^{206} would directly participate in catalysis. Substitutions of the less conserved Asp^{205} prevented the processing as well. This could indicate that the proper geometry of the residue (Asp^{205}) before the cleaved polypeptide would be essential for the processing. In line with this, His^{204} located one residue earlier could affect the geometry and activation but less efficiently than Asp^{205} does.

Inteins are typical protein structures capable of self-splicing (31). The three-dimensional structure of GyrA intein from *Mycobacterium xenopi* has been solved (32), but it is not related to Ntn hydrolases. The structure of the N-terminal cleavage site revealed that the polypeptide backbone at the cleavage site was strained due to an energetically unfavorable *cis*-peptide bond.

Our mutagenesis studies suggest that a correct conformation of residues at the cleavage site is required for the activation to take place; thus, it is possible that the polypeptide backbone is strained at the cleavage site, as was observed in the GyrA intein (32). We generated the double mutant H204G/D205G to analyze if we could decrease the tension and relax the protein backbone. This double mutant was not processed at all, which could be due to the substitution D205G as such, or the double mutant polypeptide would have a "normal" relaxed backbone geometry. Thus, the activation cleavage would be prevented in the absence of strain in the polypeptide backbone.

Activation Mechanism—A number of publications describe different reaction mechanisms for peptide bond processing. On the basis of previous studies and our mutagenesis studies, we present here a general mechanism scheme for the processing of AGA. This model could be valid for homologous enzymes and might therefore serve as a general model for the activation of enzymes in the Ntn hydrolase family.

According to the activation mechanism, the side chain of Thr^{206} would play an active role in the processing of AGA (see Fig. 9). The side chain hydroxyl group of Thr^{206} forms a hydrogen bond, and a tetrahedral intermediate is formed. After the intermediate is broken, the N-terminal peptide is released and the amino group and side chain of Thr^{206} are ready for enzymatic catalysis. This reaction mechanism would require the existence of one base and one acid that assist in the reaction. Unfortunately, so far we have not been able to identify the general base. The best candidate found for the general base in AGA crystal structure is a water molecule that is hydrogen-bonded to Asp^{237} and Thr^{206}.

In addition to being crucial for the enzymatic catalysis of AGA, the side chain of Thr^{206} has now been demonstrated to be essential to the activation cleavage. However, a more detailed understanding of the processing mechanism must wait until the structure of the precursor molecule has been solved.

Acknowledgments—We thank Tuula Manninen and Keijo Virta for excellent technical assistance. We also thank Dr. Ari Helenius for the gift of the calnexin antibody. Finally, we thank Dr. Nisse Kalkkinen, in whose laboratory the gel filtration experiments were performed.

REFERENCES

1. Brannigan, J. A., Dodson, G., Duggleby, H. J., Moody, P. C., Smith, J. L., Tomchick, D. R., and Murzin, A. G. (1995) *Nature* **378,** 416–419
2. Smith, J. L., Zaluzec, E. J., Wery, J. P., Niu, L., Switzer, R. L., Zalkin, H., and Satow, Y. (1994) *Science* **264,** 1427–1433
3. Duggleby, H. J., Tolley, S. P., Hill, C. P., Dodson, E. J., Dodson, G., and Moody, P. C. E. (1995) *Nature* **373,** 264–268
4. Löwe, J., Stock, D., Jap, B., Zwickl, P., Baumeister, W., and Huber, R. (1995) *Science* **268,** 533–539
5. Isupov, M. N., Obmolova, G., Butterworth, S., Badet-Denisot, M. A., Badet, B., Polikarpov, I., Littlechild, J. A., and Teplyakov, A. (1996) *Structure* **4,** 801–810
6. Oinonen, C., Tikkanen, R., Rouvinen, J., and Peltonen, L. (1995) *Nat. Struct. Biol.* **2,** 1102–1108
7. Zwickl, P., Kleinz, J., and Baumeister, W. (1994) *Nat. Struct. Biol.* **1,** 765–770
8. Guan, C., Cui, T., Rao, V., Liao, W., Benner, J., Lin, C.-L., and Comb, D. (1996) *J. Biol. Chem.* **271,** 1732–1737
9. Schmidtke, G., Kraft, R., Kostka, S., Henklein, P., Frömmel, C., Löwe, J., Huber, R., Kloetzel, P. M., and Schmidt, M. (1996) *EMBO J.* **15,** 6887–6898
10. Seemüller, E., Lupas, A., and Baumeister, W. (1996) *Nature* **382,** 468–471
11. Tikkanen, R., Riikonen, A., Oinonen, C., Rouvinen, R., and Peltonen, L. (1996) *EMBO J.* **15,** 2954–2960
12. Makino, M., Kojima, T., Ohgushi, T., and Yamashina, I. (1968) *J. Biochem.* (*Tokyo*) **63,** 186–192
13. Ikonen, E., Julkunen, I., Tollersrud, O-K., Kalkkinen, N., and Peltonen, L. (1993) *EMBO J.* **12,** 295–302
14. Riikonen, A., Rouvinen, J., Tikkanen, R., Julkunen, I., Peltonen, L., and Jalanko, A. (1996) *J. Biol. Chem.* **271,** 21340–21344
15. Tikkanen, R., Peltola, M., Oinonen, C., Rouvinen, J., and Peltonen, L. (1997) *EMBO J.* **16,** 6684–6693
16. Ikonen, E., Baumann, M., Gron, K., Syvänen, A. C., Enomaa, N., Halila, R., Aula, P., and Peltonen, L. (1991) *EMBO J.* **10,** 51–58
17. Peltola, M., Tikkanen, R., Peltonen, L., and Jalanko, A. (1996) *Hum. Mol. Genet.* **5,** 737–743
18. Ikonen, E., Enomaa, N., Ulmanen, I., and Peltonen, L. (1991) *Genomics* **11,** 206–211
19. Luthman, H., and Magnusson, G. (1983) *Nucleic Acids Res.* **11,** 1295–1308
20. Proia, R. L., d'Azzo, A., and Neufeld, E. F. (1984) *J. Biol. Chem.* **259,** 3350–3354
21. Halila, R., Baumann, M., Ikonen, E., Enomaa, N., and Peltonen, L. (1991) *Biochem. J.* **276,** 251–256
22. Laemmli, U. K. (1970) *Nature* **227,** 680–685
23. Tikkanen, R., Enomaa, N., Riikonen, A., Ikonen, E., and Peltonen, L. (1995) *DNA Cell Biol.* **14,** 305–312
24. Hebert, D. N., Foellmer, B., and Helenius, A. (1996) *EMBO J.* **15,** 2961–2968
25. Hammond, C., Braakman, I., and Helenius, A. (1994) *Proc. Natl. Acad. Sci. U. S. A.* **91,** 913–917
26. Peterson, J. R., Ora, A., and Helenius, A. (1995) *Mol. Biol. Cell* **6,** 1173–1184
27. Simons, J. F., Ebersold, M., and Helenius, A. (1998) *EMBO J.* **17,** 396–405
28. Xuan, J., Tarentino, A. L., Grimwood, B. G., Plummer, T. H., Jr., Cui, T., Guan, C. and van Roey, P. (1998) *Protein Sci.* **7,** 774–781
29. Fisher, K. J., Klein, M., Park, H., Vettese, M. B., and Aronson, N. N., Jr. (1993) *FEBS Lett.* **323,** 271–275
30. Riikonen, A., Tikkanen, R., Jalanko, A., and Peltonen, L. (1995) *J. Biol. Chem.* **270,** 4903–4907
31. Perler, F. B., Davis, E. O., Dean, G. E., Gimble, F. S., Jack, W. E., Neff, N., Noren, C. J., Thorner, J., and Belfort, M. (1994) *Nucleic Acids Res.* **22,** 1125–1127
32. Klabunde, T., Sharma, S., Telenti, A., Jacobs, W. R. J., and Sacchettini, J. C. (1998) *Nat. Struct. Biol.* **5,** 31–36
33. McRee, D. E. (1992) *Mol. Graph.* **10,** 44–46
34. Nicholls, A., Sharp, K. A., and Honig, B. (1991) *Proteins* **11,** 281–296